Intrinsic mutant HTT-mediated defects in oligodendroglia cause myelination deficits and behavioral abnormalities in Huntington disease

Intrinsic mutant HTT-mediated defects in oligodendroglia cause myelination deficits and behavioural abnormalities in Huntington disease

Costanza Ferrari Bardile[1], Marta Garcia-Miralles[1], Nicholas Caron[2], Nirmala Rayan[1], Sarah Langley[3], Nathan Harmston[4], Ana Maria Rondelli[5], Roy Teo[1], Sabine Waltl[2], Lisa Anderson[2], Han-Gyu Bae[1], Sangyong Jung[1], Anna Williams[6], Shyam Prabhakar[7], Enrico Petretto[3], Michael Hayden[2], Mahmoud A Pouladi[1]

[1]Agency for Science, Technology and Research, [2]University of British Columbia, [3]Duke NUS Graduate Medical School, [4]Duke-NUS, [5]MS Centre, Centre for Regenerative Medicine, University of Edinburgh, [6]MS Centre, Centre for Regenerative Medicine, University of Edinburgh, Edinburgh, UK, [7]Genome Institute of Singapore

Submitted to Proceedings of the National Academy of Sciences of the United States of America

White matter abnormalities are a nearly universal pathological feature of neurodegenerative disorders including Huntington disease (HD). A long-held assumption is that this white matter pathology is simply a secondary outcome of the progressive neuronal loss that manifests with advancing disease. Using a mouse model of HD, here we show that white matter and myelination abnormalities are an early disease feature appearing before the manifestation of any behavioural abnormalities or neuronal loss. We further show that selective inactivation of mutant huntingtin (mHTT) in the NG2+ oligodendrocyte progenitor cell population prevented myelin abnormalities and certain behavioural deficits in HD mice. Strikingly, the improvements in behavioural outcomes were seen despite the continued expression of mHTT in non-oligodendroglial cells including neurons, astrocytes and microglia. Using RNA-seq and ChIP-seq analyses, we implicate a novel pathogenic mechanism, namely enhancement of PRC2 (polycomb repressive complex 2) activity by mHTT, in the intrinsic oligodendroglial dysfunction and myelination deficits observed in HD. Our findings challenge the long-held dogma regarding the etiology of white matter pathology in HD and highlight the contribution of epigenetic mechanisms to the observed intrinsic oligodendroglial dysfunction. Our results further suggest that ameliorating white matter pathology and oligodendroglial dysfunction may be beneficial for HD.

Huntington disease | white matter | oligodendrocytes | myelination | PRC2

Introduction

White matter (WM) structures are profoundly affected in nearly all neurodegenerative disorders. In Huntington disease (HD), morphometric and histological studies have shown myelin breakdown and loss of white matter volume in post mortem HD brains (1-3). Furthermore, structural magnetic resonance and diffusion tensor imaging (MRI) have revealed volumetric atrophy and tract connectivity abnormalities in white matter regions in pre-symptomatic gene carriers and symptomatic patients with HD (4-6). Evidence of white matter abnormalities has also been observed in animal models of HD. Indeed, decreased expression in myelin binding protein (MBP) and thinner myelin sheaths were found in the BACHD mouse model of HD at a very early time point, weeks before the onset of behavioral phenotypes (7). In agreement with this, our laboratory has recently shown white matter microstructural abnormalities, thinner myelin sheaths and a lower expression of myelin related genes in the YAC128 mouse model of HD at a very early age (8, 9). Despite this prominence of white matter atrophy in HD, its etiology is not fully understood. It has long been assumed that white matter atrophy is secondary to neuronal loss. However, the appearance of white matter abnormalities very early in the disease course, indeed many years before neurological onset in patients (6, 10, 11) and prior to any neuronal loss in animal models of HD (7, 8, 12) suggests otherwise. Oligodendrocytes, the myelinating cells of the central nervous system (CNS), play a crucial role in maintaining axonal integrity and function. Deficits in oligodendrocytes or their precursors can lead to axonal pathology and neurodegeneration (13). Here, we hypothesized that intrinsic mHTT-mediated deficits in oligodendroglia contribute to myelination abnormalities and behavioural manifestations in HD. To test this hypothesis, we evaluated the impact of genetic reduction of mHTT in the oligodendrocyte progenitor cell (OPC) population specifically on myelination and behavioural phenotypes in HD mice.

Results

NG2Cre mediated reduction of m*HTT* in oligodendroglia

BACHD mice carry a full-length human mutant *HTT* gene modified to harbor a *loxP*-flanked exon 1 sequence (14). By crossing BACHD to NG2Cre mice which express the Cre recombinase in NG2+ OPCs (Fig. 1A), we were able to reduce mHTT expression specifically in oligodendroglia. Genomic PCR analysis showed successful excision of m*HTT* in the cortex of BACHDxNG2Cre (BN) mice (Fig. 1B). We further confirmed

Significance

Huntington disease (HD) is a progressive neurodegenerative disorder. While research efforts in HD have largely focused on understanding grey matter atrophy representing neuronal loss, there is clear evidence from human and animal studies that white matter structures, representing myelin-rich regions of the brain, are profoundly affected. Here, using an HD animal model, we show that myelin abnormalities appear before the manifestation of behavioural deficits or neuronal loss. Reduction of the mutant protein in oligodendrocytes, the myelinating cells of the central nervous system, prevented myelin abnormalities and certain behavioural deficits in HD mice. Our data implicate a novel pathogenic mechanism and suggest that directly targeting white matter pathology could be beneficial for HD. New therapeutic interventions targeting oligodendroglia should be considered.

Reserved for Publication Footnotes

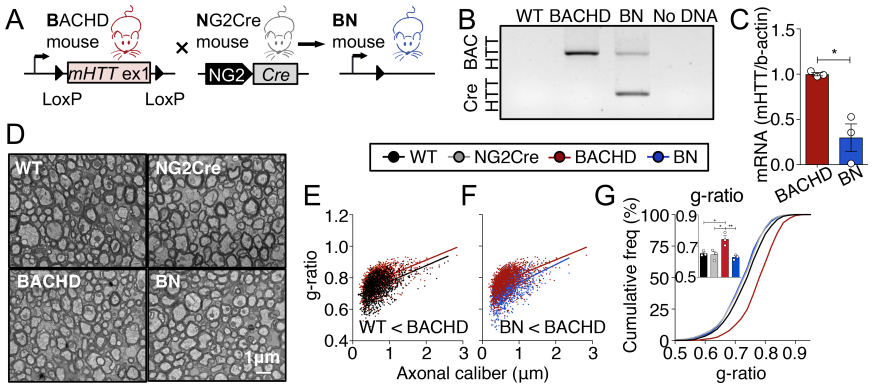

Fig. 1. OPC-intrinsic effects of mHTT cause myelination abnormalities in HD mice.(A) Schematic representation of Cre-mediated genetic reduction of mHTT expression in OPCs (NG2+ cells) in BACHD mice. (B) PCR analysis confirmed the excision of human mHTT exon 1 in the cortex of BN mice. (C) mHTT mRNA levels are reduced in purified OPCs in BN mice at P6-P7. n = 3/genotype ($P = 0.0100$, t = 4.601, d.f. = 4). (D) EM images of myelinated axons in the CC at 12 months of age. Scale bar represents 1 µm. (E-G) Higher g-ratios (thinner myelin sheaths) in BACHD mice are rescued in BN mice. n = 3/genotype; ~300 axons quantified per animal. Data show means ± SEM; P * < 0.05, ** P < 0.01; two-tailed Student's test in C and one-way ANOVA followed by Tukey's test in G.

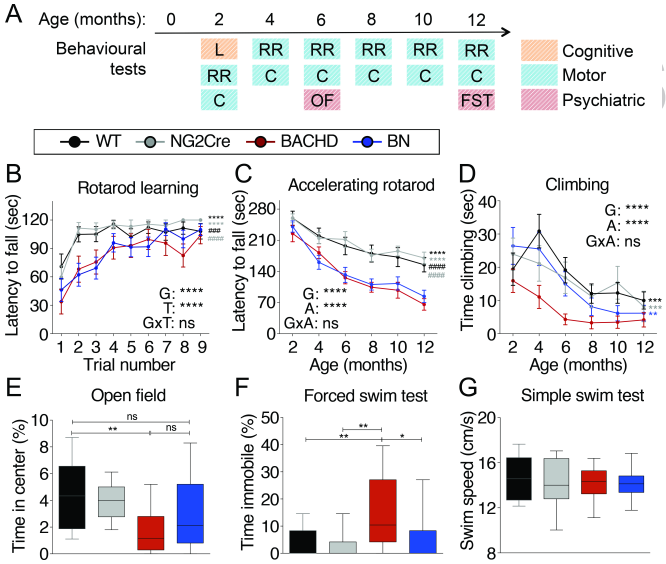

Fig. 2. Behavioural deficits in HD mice are partly the result of mHTT-mediated defects in oligodendroglia. (A) Overview of behavioural assessments. BACHD mice show cognitive deficits in the rotarod learning (B), motor deficits in the rotarod (C) and climbing (D) tests, anxiety-like behavior in the OF at 6 months of age (E) and depressive-like behavior in the Porsolt FST at 12 months of age (F). The ability to swim is comparable among genotypes at 12 months of age (G).BN mice show a rescue in some of the behavioral phenotypes. n = 12-20 mixed gender/genotype. Data represent means ± SEM; ns = not significant; * P < 0.05; ** P < 0.01; *** P < 0.001; **** P < 0.0001 (compared to BACHD); ### P < 0.001; #### P < 0.0001 (compare to BN). One-way ANOVA (E-G) or two-way ANOVA (B-D) followed by Tukey's multiple comparisons test were applied for all behavioral studies. G=genotype, T=trial, A=age.

that m*HTT* mRNA levels in isolated NG2+ OPCs were reduced by ~70% in BN mice (Fig. 1C).

OPC-intrinsic effects of mHTT cause myelin deficits in HD mice

To assess the impact of reducing m*HTT* expression specifically in OPCs on myelination deficits in HD, we used electron microscopy to visualize myelinated fibres in the corpus callosum, the largest white matter structure in the brain, at 12 months of age (Fig. 1D). We examined g-ratios of myelinated axons, a measure of myelin sheath thickness calculated as the ratio of axon diameter (axon caliber) to myelinated fibre diameter. BACHD mice presented increased g-ratio compared with WT (Fig. 1E), indicating that their myelin sheaths were thinner. We found that selective reduction of m*HTT* in OPCs reversed this phenotype in BN mice (Fig. 1F). Indeed, the increased mean g-ratio in BACHD mice was rescued in BN mice, where it was comparable to WT mice (Fig. 1G). We also performed the same analysis at one month of age (*SI Appendix*, Fig. S1A), where no significant differences in g-ratio were found among genotypes with one-way ANOVA. However, a binary t-test of only WT and BACHD groups showed increased mean g-ratio in BACHD mice (*SI Appendix*, Fig. S1, B and C). This indicates that myelin sheaths in BACHD mice were thinner compared with WT mice as early as one month of age, demonstrating that myelin abnormalities in HD are an early phenotype. Periodicity, a measure of myelin compaction calculated as the mean distance between two major dense lines, was also increased in BACHD mice indicating less compact myelin compared with WT mice (*SI Appendix*, Fig. S1D and E). Both abnormalities, mean g-ratio and periodicity, were rescued in BN mice (*SI Appendix*, Fig. S1, B-E). We next analyzed the number of myelinated axons in the corpus callosum (CC) and did not find any significant differences between the genotypes, suggesting no defects in the initiation of myelination (*SI Appendix*, Fig. S1F). To evaluate the functional impact of the WM abnormalities, we measured compound action potentials (CAPs) in the CC of BACHD brain slices at 14 months of age. Quantification of the average stimulus-response revealed a modest decrease in the amplitude of the N1 component (myelinated axons), but not N2 (unmyelinated), in BACHD mice compared with WT mice, although the difference did not reach statistical significance (*SI Appendix*, Fig. S2B). BN mice showed a similar amplitude of the N1 component to WT mice (*SI Appendix*, Fig. S2, A and B). Furthermore, a modest but not significant decrease in the area of CAPs was detected on BACHD and BN in both N1 and N2 components, while duration of CAPs was comparable between the groups (*SI Appendix*, Fig. S2, C and D). The findings of the electron microscopy myelin sheath analyses clearly indicate that intrinsic oligodendroglial dysfunction mediated by mHTT contributes to structural myelination defects in HD. However, a conclusion of how this dysfunction impacts conduction velocity cannot be drawn due to the small sample size.

Behavioural deficits in HD mice are partly the result of mHTT-mediated defects in oligodendroglia

We next tested whether specific inactivation of m*HTT* in OPCs leads to improved motor and psychiatric-like behavioral phenotypes in BACHD mice. We evaluated mice at 2, 4, 6, 8, 10 and 12 months of age using a battery of behavioural tests

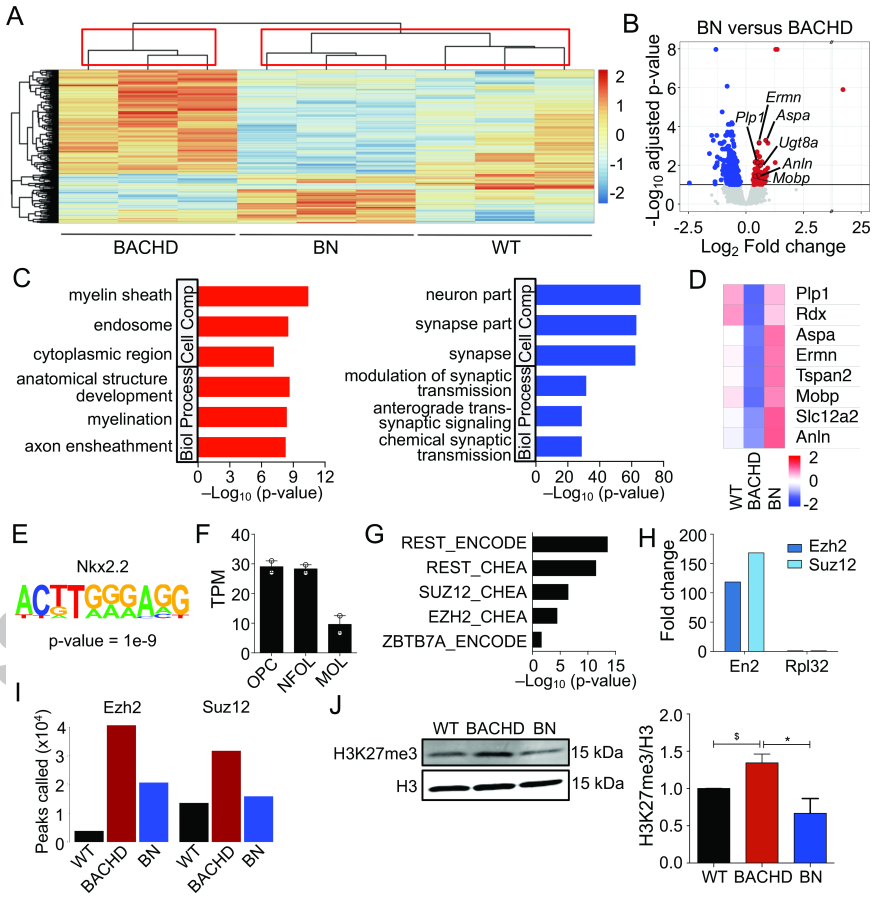

Fig. 3. Epigenetic dysregulation mediates mHTT effects on oligodendroglia. **(**A) Heatmap and hierarchal clustering of the significantly differentially expressed genes between WT (n=3), BACHD (n=3), and BN (n=3) (360 genes, 10% FDR LRT). Red indicates higher gene expression and blue represents lower gene expression. Boxes indicate clusters of samples determined by 10,000 bootstraps (B) Volcano plot showing the differentially expressed genes between BN (n=3) and BACHD (n=3) mice corpus callosum. The significant up-regulated genes with respect to BN are indicated in red, while the significant down-regulated genes are indicated in blue (FDR<10%). (C) GO analysis of significant DEGs between BACHD and BN mice. The top three significant terms (FDR<5%) for up-regulated and down-regulated genes are shown. (D) Heat maps shows mean gene expression levels of selected genes in WT, BACHD and BN mice. (E) Nkx2.2 appears as top motif enriched in up-regulated DEGs between BACHD and BN. (F) *Htt* gene expression (Fragments Per Kilobase Million, FPKM) in different stages of oligodendroglial differentiation (from (20), n=2 for each group, bars indicate mean). OPC = oligodendrocyte progenitor cells, NFOL = newly formed oligodendrocytes, MOL = myelinating oligodendrocytes. (G) REST and PRC2 binding sites are enriched in DEGs between BACHD and BN. (H) ChIP-qPCR enrichment at the *En2* promoter in CC for EZH2 and SUZ12. Rpl32 was used as negative control. (I) Increased number of EZH2 and SUZ12 binding sites in the BACHD compared to WT is partially rescued in BN mice. (J) Immunoblot analysis of H3K27me3 in the CC of WT, BACHD, and BN mice. Values normalized to WT and presented as means ± SEM; n=3 per genotype; * $P < 0.05$ by one-way ANOVA with Tukey's post-hoc test; $ $P < 0.05$ by unpaired two-tailed t-test.

(Fig. 2A). BACHD mice exhibited motor deficits as early as four months of age in the rotarod (latency to fall) and climbing (time climbing) tests, both reliable assays of motor impairment in BACHD mice (15). We found that BN mice showed improvements in the climbing test but not rotarod training or performance (Fig. 2, B-D). The improvements in climbing performance of BN mice are most readily seen at 2-6 months, with more comparable performance amongst the groups at later time-points due to age-dependent decline in the WT and BN groups. BACHD mice also displayed psychiatric-like behavioral deficits, including anxiety-like behavior in the open-field (OF) test at six months of age and depressive-like behavior in the Porsolt forced swim (FST) test at 12 months of age, as shown previously (15). BN mice showed a modest improvement in the OF test, where the time spent in the center is not significantly different compared to WT mice, and a significant improvement in the FST (Fig. 2E and F). In order to verify that this phenotype reflects psychiatric-like behavior rather than motor impairments, we tested the mice for swimming ability in a simple swim test. We showed that the ability to swim is comparable among genotypes (Fig. 2G).

To rule out the possibility that increased body weight may contribute to certain behavioural phenotypes, body weight was plotted against time climbing and time in center of OF at 6 months of age, and time immobile at 12 months of age. Regression analysis revealed no correlation between body weight and climbing time (r2 = 0.10, $P = 0.24$ for WT; r2 = 0.01, $P = 0.72$ for NG2; r2 = 0.01, $P = 0.74$ for BACHD; r2 = 0.02, $P = 0.55$ for BN), body weight and time in center (r2 = 0.02, $P = 0.57$ for WT; r2 = 0.01, $P = 0.72$ for NG2; r2 = 0.09, $P = 0.31$ for BACHD; r2 = 0.12, $P = 0.13$ for BN), and body weight and time immobile (r2 = 0.15, $P = 0.17$ for WT; r2 = 0.15, $P = 0.17$ for NG2; r2 = 0.004, $P = 0.82$ for BACHD; r2 = 0.04, $P = 0.39$ for BN), showing that increased body weight is not contributing to these behavioural phenotypes.

Therefore, selective inactivation of m*HTT* in OPCs improves certain aspects of motor and psychiatric-like deficits in BACHD mice, suggesting that mHTT-related effects in oligodendroglia contribute to the manifestation of some behavioural phenotypes in HD.

Absence of OPC-intrinsic effects of mHTT on neuropathology and oligodendrogenesis in HD mice

We next addressed whether the specific inactivation of m*HTT* in OPCs can influence striatal atrophy in BACHD mice. We found that striatal volume was decreased in BACHD mice (*SI Appendix*, Fig. S3B) while forebrain weight was not significantly different among genotypes by one-way ANOVA. However, when a binary t-test was used, BACHD mice showed a significant decrease in forebrain weight compared to WT (*SI Appendix*, Fig. S3A). Forebrain weight and striatal volume loss were not rescued in BN mice (*SI Appendix*, Fig. S3, A and B), suggesting that striatal pathology is not markedly impacted by mHTT-related oligodendroglial deficits.

Changes in the proliferation of NG2+ cells are observed in a wide variety of acute and chronic CNS conditions (16). To investigate whether oligodendroglia proliferation is altered in HD, we counted the number of cells that were positive for Olig2 (a transcription factor that marks the entire oligodendrocyte lineage), together with BrdU in the CC (*SI Appendix*, Fig. S3C). We also evaluated oligodendroglia density using Olig2, GST-pi (a marker of mature oligodendrocytes) and PDGFRα (an OPC marker) cell markers (*SI Appendix*, Fig. S3D). No changes were observed in oligodendroglia density or their proliferation in BACHD mice at 12 months of age, suggesting that myelin pathology in BACHD mice is not associated with altered oligodendroglial proliferation or differentiation in adult mice. Also, we did not find any differences in the density or proliferation of oligodendroglia populations in the striatum and subventricular zone in BACHD mice compared with WT mice (*SI Appendix*, Fig. S3, E-H).

RNA-seq analysis provides insights into the pathogenic mechanisms

To gain insights into the pathogenic mechanisms underlying the oligodendrocyte dysfunction observed in HD mice, we performed RNA-seq analysis on the CC of WT, BACHD and BN mice at one month of age. We compared the gene expression profiles of the three genotypes and identified 360 significantly differentially expressed genes (DEGs, FDR 10%). Hierarchical clustering of the gene expression from these DEGs revealed that the expression profile from BN mice was significantly closer to that of the WT mice than that of the BACHD mice ($P<0.05$, Fig. 3A, Dataset S1).

We then compared gene expression profiles from BN and BACHD only and identified 449 DEGs (FDR<10%, Fig. 3B; Dataset S1). Functional annotation of these DEGs revealed increases in the expression of key genes associated with myelination in BN mice versus synaptic transmission in BACHD mice (Fig. 3C; Dataset S2). A heatmap of representative myelin related genes that were down-regulated in BACHD compared to WT mice and up-regulated in BN mice is shown in Fig. 3D. We also found that some myelin proteins such as Ermin, MBP (myelin basic protein), MAG (myelin-associated glycoprotein) and Septin-8 were indeed more highly expressed in BN versus BACHD mice (*SI Appendix*, Fig. S4, A-D). To examine whether certain DNA motifs were enriched in the DEGs, we applied a motif-discovery algorithm, HOMER (17). An Nkx2.2 consensus-binding motif, ACTTGGGAGG, was the top motif enriched among genes up-regulated in BN mice (Fig. 3E, *SI Appendix*, Table S1). Nkx2.2 plays a key role in the regulation of OPC differentiation (18) and is up-regulated during the OPC-to-oligodendrocyte transition (19). Interestingly, *Htt* is more highly expressed in OPCs and newly formed oligodendrocytes compared with more mature, myelinating oligodendrocytes (Fig. 3F) (20), suggesting the possibility of greater influence of mutant HTT in OPCs and newly differentiated oligodendrocytes.

To further investigate the transcriptional changes identified, we performed transcription-factor/target-gene interactions analysis using ChEA, a database of ChIP-based studies (21). We found that DEGs between BACHD and BN were enriched for RE1 Regulation Transcription Factor (REST) and Polycomb Repressive Complex 2 (PRC2) binding sites (Fig. 3G). Dysregulation of REST has been implicated in HD, where as a result of derepression by mutant HTT it translocates from the cytoplasm to the nucleus in neurons leading to the repression of key neuronal genes such as *BDNF* (22). In OPCs, REST is required for the repression of neuronal properties and their development into oligodendrocytes (23). Here, however, the role of mHTT in REST dysregulation is not clear. PRC2 is a class of polycomb-group proteins (PcG) thought to play a key role in the initiation of gene repression (24). Via EZH2, the catalytic subunit of the complex, PRC2 initiates repressive activity at target gene promoters by trimethylating histone H3 lysine 27 (H3K27me3). PRC2 plays a major role in lineage determination and cell type specification, including oligodendroglia differentiation (25). PRC2 activity is indeed down-regulated at the earliest stages of neuron and astrocyte differentiation, while down-regulation of PRC2 activity in oligodendrocytes parallels their maturation (25). HTT is known to interact with and stimulate PRC2 activity in a polyglutamine length-dependent manner (26). Moreover, mHTT enhances PRC2 activity, increasing PRC2-specific histone H3K27 methylation. Here we propose a mechanism by which mHTT, enhancing PRC2 activity in oligodendroglia, leads to a delay in their maturation and results in myelination defects. In order to test the hypothesis of increased PRC2 activity in oligodendrocyte-enriched white matter regions as a result of mHTT, we performed chromatin immunoprecipitation followed by sequencing (ChIP-seq) analysis on the CC of WT, BACHD and BN mice at one month of age for EZH2, and SUZ12 (a subunit of PRC2).

Epigenetic dysregulation contributes to mHTT-mediated defects in oligodendroglia

We first carried out ChIP-qPCR analysis, which showed high enrichment (EZH2 and SUZ12 occupancy) at the promoter of En2, a known target, compared to Rpl32 (negative control), in the CC of WT mice (Fig. 3H). ChIP-seq revealed an increased number of EZH2 and SUZ12 binding sites in BACHD compared with WT chromatin (Fig. 3I). We found that the increased EZH2 and SUZ12 peaks observed in BACHD mice are rescued in BN mice (Fig. 3I), implicating a role for excessive PRC2 activity in oligodendroglial dysfunction in HD. EZH2 and SUZ12 binding site peaks significantly overlapped in WT, BACHD and BN conditions (*SI Appendix*, Fig. S5A). Enrichment analysis revealed that peaks with significantly higher binding of SUZ12 in BACHD compared to BN were enriched for processes including cerebellum development, the node of Ranvier and a number of processes associated with differentiation and morphogenesis (*SI Appendix*, Fig. S5B). EZH2 peaks with higher binding in BACHD versus BN were enriched for similar processes including regulation of myelination and axonogenesis. *Plekhb1*, a gene highly expressed in myelin (27), was down-regulated in BACHD compared to BN (nominal p-value < 0.05), and was found to only have an EZH2 peak close to its TSS in BACHD and not in WT or BN (*SI Appendix*, Fig. S5D).

We compared the set of genes whose promoters (± 5kb from the TSS) were differentially bound by EZH2 between BN and BACHD (Dataset S3) with the set genes identified as differentially expressed between BN and BACHD. We found that the set of DEGs was significantly enriched for differential EZH2 binding in their promoters (11% of DEGs, $P=0.001$, Chi-squared test). These differentially bound DEGs included genes involved in myelination such as Semaphorin-4D (Sema4d) (28). In contrast, the set of DEGs between BN and WT showed no enrichment for differential binding of EZH2 (7% of DEGs, $P=0.40$, Chi-squared test). Differential binding of SUZ12 in the promoter regions (Dataset S3) did not show an enrichment in the set of DEGs. Finally, we assessed the levels of H3K27me3 in the CC of WT, BACHD, and BN mice as a global measure of PRC2 activity.

Consistent with the ChIP-seq results, we found that the elevated levels of H3K27me3 in BACHD mice are rescued in BN mice (Fig. 3J). These results implicate differences in the binding and activity of PRC2, driven by mHTT, in the dysregulation of key genes involved in oligodendrocyte myelination.

Discussion

In this study, we provide strong evidence for intrinsic mutant HTT-mediated defects in oligodendroglia leading to myelination deficits and behavioural abnormalities in HD, and contributing to the overall pathology of HD. Consistent with previous studies on animal models of HD (7, 8), we show that BACHD mice exhibit thinner myelin and decreased myelin compaction as early as one month of age, suggesting that myelin abnormalities in HD are an early phenotype. The appearance of white matter abnormalities early in the disease course is in agreement with clinical studies, where it appears many years before neurological onset in patients (6, 10). We show that these early phenotypes worsen with age, with greater myelin thinning in BACHD mice at 12 months old, indicating that myelin structure deteriorates with disease progression, in line with the worsening of WM pathology in subjects with HD as the disease progresses (10). While myelination abnormalities in HD have long been considered to be a secondary effect of axonal degeneration, here we show that these are primarily driven by intrinsic oligodendroglial dysfunction in early stages of disease and are rescuable by inactivating m*HTT* in oligodendroglia.

WM abnormalities have been linked to neuropsychiatric disorders, including HD (29) and major depression (30-32), where disconnection of WM regions including the CC has been reported. In addition, loss of NG2-expressing glial cells has been shown to trigger depressive-like behaviours in mice (33). Motor and cognitive abnormalities have also been associated with changes in white matter structure in several disorders including HD (34, 35). Our observations of improved psychiatric-like phenotypes, such as a rescue in the FST, and motor function that accompanied the improvements in myelination (e.g. rescue of increased callosal g-ratios) in BN mice support this link between WM abnormalities and neurological deficits.

While inactivation of m*HTT* in oligodendroglia rescues myelin deficits and ameliorates certain aspects of behavioural phenotypes, it is not sufficient alone to improve striatal neuropathology in HD mice. This lack of rescue of striatal atrophy may not be entirely surprising given that mutant HTT remains expressed in neurons and other glial cell types, and thus continues to exert its detrimental effects on the function and survival of striatal neurons. Moreover, medium spiny neurons, which are the major neuronal population in the striatum and most vulnerable neurons in HD (36), have very short projections and are mostly unmyelinated, and thus may not benefit directly from improved oligodendroglial function.

Two mechanisms that underlie myelination deficits in HD have been proposed: abnormal cholesterol metabolism (7) and MYRF (myelin regulator factor) dysregulation by its abnormal association with mHTT (37). MYRF regulates oligodendrocyte maturation and is essential for proper myelination (38). Reduction of MYRF transcriptional activity has been associated with oligodendroglial dysfunction and myelin impairment in HD (37). Decreased cholesterol biosynthesis has been linked to impaired activity of peroxisome-proliferator-activated receptor gamma coactivator 1 alpha (PGC1α) in HD (7). Here we implicate enhancement of PRC2 activity by mHTT in intrinsic oligodendroglial dysfunction and myelination deficits in HD, highlighting the contribution of epigenetic mechanisms to HD white matter pathology. Oligodendroglia development is regulated by a dynamic interaction between genetic and epigenetic factors. EZH2, a component of PRC2, is a histone methyltransferase that, through the methylation of lysine 27 on histone H3 (H3K27), plays a crucial role in oligodendroglia lineage determination (25). A number of compounds have been developed to dampen PRC2 function by inhibiting the enzymatic activity of EZH2 (39). Targeting PRC2 activity with such EZH2 antagonists would help address whether reducing PRC2 activity could lead to improvements in myelination deficits in HD. Given its broad activity and ubiquitous expression, however, it is doubtful that targeting general PRC2 activity would be a viable therapeutic strategy for HD. Nonetheless, efforts to establish the basis of interaction between mutant HTT and PRC2 may reveal novel strategies for moderation of HTT's interaction with PRC2 and normalization of its activity. Such targeted mutant HTT-specific approaches have the potential to provide therapeutic benefit while at the same time minimizing undesirable side-effects.

While not validated in the current study, our analysis also highlights a potential role for dysregulation of Nkx2.2 target genes in the myelination deficits in HD. Of note, a recent human pluripotent stem cell-based study has provided evidence that transcriptional targets of Nkx2.2 are down-regulated in HD oligodendroglia compared with control (40). These studies together with our findings indicate a role for deficits in multiple oligodendroglia processes as primary contributors to myelination abnormalities in HD. However, the degree of interdependence and the relative contribution of the different pathways identified to WM pathology in HD remains to be determined.

Emerging evidence suggests that neurodevelopment may be altered in HD (41), including several aspects related to oligodendroglia. For example, mice expressing reduced levels of Htt throughout development exhibit OPC maturation abnormalities and white matter tract impairments (42). OPCs isolated from neonatal HD mouse brains and derivative oligodendrocytes show deficits in the levels of myelin-related genes (8). Mouse HD embryonic stem cells show altered oligodendrogenesis upon neural induction (43), and OPCs derived from human HD embryonic stem cells show dysregulation in myelin-related transcriptional profiles as well as altered myelination properties (40). Our observations of early post-natal deficits in myelination (e.g. as early as 1 months of age) are in line with the possibility that the myelination deficits in HD originate during development and persist with age. An outstanding question that remains, particularly in the context of the HTT lowering therapeutic efforts currently underway, is whether inactivating mutant HTT in mature oligodendrocytes in adulthood would rescue the myelination abnormalities and associated neurological deficits.

In addition to oligodendroglia in the CNS, NG2 is also expressed by Schwann cells in the peripheral nervous system (44). Although in the few studies that have examined Schwann cells in HD, they were found to be unaffected (45), their possible role in the current study was not evaluated. Future studies to investigate possible Schwann cell pathology and any relationship to disease manifestations in HD should be considered.

A better understanding of the mechanisms underlying myelination deficits could shed light on new therapeutic approaches for HD. Strategies for intervention should be expanded from the current neuro-centric focus of most therapeutic efforts to include oligodendroglial targets. Indeed, our data suggests that directly targeting white matter pathology could be beneficial for HD.

Materials and methods

Animals

BACHD SPF mice (JAX, Stock Number: 008197) were maintained on the FVB/N background. NG2-Cre SPF mice (JAX, Stock Number: 008533) were backcross onto the FVB/N background and then bred to generate BACHD-NG2Cre mice. Cre-excision validation was performed by PCR on genomic DNA using primers listed in Table S2. For details, see *SI Appendix.*

PCR for Cre-excision validation

Genomic DNA was extracted from dissected frozen mouse cortex at 1 month of age using the DNeasy Tissue kit (Qiagen). To visualize the successful deletion of HTT exon 1 in BACHDxNG2Cre mice the PCR products were run

on a 1% agarose gel with SYBER Safe DNA gel stain (Invitrogen). The primers flanking the loxP sites of HTT exon 1 in the BACHD mice are summarized in Table S2.

Real-time quantitative PCR

Brains from P6-P7 pups were collected and dissociated with the Neural Tissue Dissociation Kit (Miltenyi Biotec). A pure population of NG2+ OPCs was isolated using anti-AN2 magnetic microbeads (Miletenyi Biotec) through MACS separation. For details, see *SI Appendix.*

Transmission electron microscopy

Mice were transcardially perfused with 2.5% glutaraldehyde and 2.5% PFA in phosphate buffer saline before post-fixing the brains overnight at 4°C in the same buffer. Brains were subsequently washing in PBS and transferred in 5% sucrose plus 0.08% NaN3 in PBS. For details, see *SI Appendix.*

Corpora callosa slice preparation and electrophysiology

14 months old female mice were used for this experiment. Animals brain were carefully dissected after cervical dislocation and placed in oxygenated (95% O2 + 5% CO2) ice-cold sucrose artificial cerebrospinal fluid (ACSF) cutting solution For details and for the compound action potentials (CAPs) recording, see *SI Appendix.*

Behavioural test of affective function

All the behavioural tests were performed during the dark phase of the reverse light/dark-cycle. One independent cohort was used with n = 12-20 mixed gender per genotype (body weight in grams ± SD: 20.56 ± 3.15 in WT, 20.28 ± 3.54 in NG2Cre, 24.16 ± 3.47 in BACHD and 19.99 ± 3.23 in BN at 6 weeks). For details, see *SI Appendix*.

Immunohistochemistry and stereological measurements

For immunohistochemistry and stereological measurements one independent cohort was used with n = 13-18 per genotype. For cell proliferation studies, 200mg/kg of BrdU (Sigma, B9285) was injected intraperitoneally for 3 days at 12 h intervals before transcardial perfusion with 4% PFA and brain extraction. For details and antibodies used, see *SI Appendix.*

Protein analysis

Protein lysate of CC from male mice were prepared using RIPA buffer (Sigma-Aldrich) with 1mM PMSF (Sigma-Aldrich), 5µm Z-VAD (Promega), 1mM NaVan (Sigma-Aldrich), and 1x Complete Protease Inhibitor Cocktail tablets (Roche). For details and antibodies used, see *SI Appendix.*

RNA-seq and ChIP-seq analysis

RNA was extracted from mouse CC (WT, n=3; BACHD, n=3; BN, n=3) using Trizol (Life Technologies) and subsequently a RNeasy plus mini kit (Qiagen) according to the manufacturer's instructions. For ChIP-seq analysis mouse CC tissues were microdissected and pooled from 12 mice per sample at 1 month of age. For details on RNA-seq and ChIP-seq analysis, see *SI Appendix.*

Acknowledgements

We thank members of the Pouladi lab for helpful discussions and comments. C.F.B. is supported by a Singapore International Graduate Award (SINGA) from the A*STAR. M.A.P. is supported by grants from A*STAR, and the National University of Singapore, Singapore. **Competing interests** The authors declare no competing financial interests. **Author contributions** CFB and MAP developed the study, conceived the experimental plans, and analyzed the data. CFB, RTYT, SJ, HGB, MGM, NSC, SW and LMA performed experiments. SRL and NAR performed the bioinformatics analysis. AMR, AW, SP, EP and MRH provided intellectual input. CFB and MAP interpreted the data and wrote the manuscript. All authors read and edited the manuscript.

1. la Monte de SM, Vonsattel JP, Richardson EP (1988) Morphometric demonstration of atrophic changes in the cerebral cortex, white matter, and neostriatum in Huntington's disease. *J Neuropathol Exp Neurol* 47(5):516–525.
2. Mann DMA, Oliver R, Snowden JS (1993) The topographic distribution of brain atrophy in Huntington's disease and progressive supranuclear palsy. *Acta Neuropathol* 85(5). doi:10.1-007/BF00230496.
3. Bartzokis G, et al. (2007) Myelin breakdown and iron changes in Huntington's disease: pathogenesis and treatment implications. *Neurochem Res* 32(10):1655–1664.
4. Reading SAJ, et al. (2005) Regional white matter change in pre-symptomatic Huntington's disease: a diffusion tensor imaging study. *Psychiatry Res* 140(1):55–62.
5. Rosas HD, et al. (2006) Diffusion tensor imaging in presymptomatic and early Huntington's disease: Selective white matter pathology and its relationship to clinical measures. *Mov Disord* 21(9):1317–1325.
6. Rosas HD, et al. (2018) Complex spatial and temporally defined myelin and axonal degeneration in Huntington disease. *Neuroimage (Amst)* 20:236–242.
7. Xiang Z, et al. (2011) Peroxisome-proliferator-activated receptor gamma coactivator 1 α contributes to dysmyelination in experimental models of Huntington's disease. *J Neurosci* 31(26):9544–9553.
8. Teo RTY, et al. (2016) Structural and molecular myelination deficits occur prior to neuronal loss in the YAC128 and BACHD models of Huntington disease. *Hum Mol Genet* 25(13):2621–2632.
9. Garcia-Miralles M, et al. (2018) Laquinimod Treatment Improves Myelination Deficits at the Transcriptional and Ultrastructural Levels in the YAC128 Mouse Model of Huntington Disease. *Mol Neurobiol* 130:1759.
10. Tabrizi SJ, et al. (2009) Biological and clinical manifestations of Huntington's disease in the longitudinal TRACK-HD study: cross-sectional analysis of baseline data. *Lancet neurology* 8(9):791–801.
11. Paulsen JS, et al. (2008) Detection of Huntington's disease decades before diagnosis: the Predict-HD study. *J Neurol Neurosurg Psychiatr* 79(8):874–880.
12. Carroll JB, et al. (2011) Natural history of disease in the YAC128 mouse reveals a discrete signature of pathology in Huntington disease. *Neurobiol Dis* 43(1):257–265.
13. Nave K-A (2010) Myelination and support of axonal integrity by glia. *Nature* 468(7321):244–252.
14. Gray M, et al. (2008) Full-length human mutant huntingtin with a stable polyglutamine repeat can elicit progressive and selective neuropathogenesis in BACHD mice. *J Neurosci* 28(24):6182–6195.
15. Pouladi MA, et al. (2012) Marked differences in neurochemistry and aggregates despite similar behavioural and neuropathological features of Huntington disease in the full-length BACHD and YAC128 mice. *Hum Mol Genet* 21(10):2219–2232.
16. Levine JM, Reynolds R, Fawcett JW (2001) The oligodendrocyte precursor cell in health and disease. *Trends Neurosci* 24(1):39–47.
17. Heinz S, et al. (2010) Simple combinations of lineage-determining transcription factors prime cis-regulatory elements required for macrophage and B cell identities. *Mol Cell* 38(4):576–589.
18. Qi Y, et al. (2001) Control of oligodendrocyte differentiation by the Nkx2.2 homeodomain transcription factor. *Development* 128(14):2723–2733.
19. Hu BY, Du ZW, Li XJ, Ayala M, Zhang SC (2009) Human oligodendrocytes from embryonic stem cells: conserved SHH signaling networks and divergent FGF effects. *Development* 136(9):1443–1452.
20. Zhang Y, et al. (2014) An RNA-sequencing transcriptome and splicing database of glia, neurons, and vascular cells of the cerebral cortex. *J Neurosci* 34(36):11929–11947.
21. Lachmann A, et al. (2010) ChEA: transcription factor regulation inferred from integrating genome-wide ChIP-X experiments. *Bioinformatics* 26(19):2438–2444.
22. Zuccato C, et al. (2003) Huntingtin interacts with REST/NRSF to modulate the transcription of NRSE-controlled neuronal genes. *Nature Genetics* 35(1):76–83.
23. Dewald LE, Rodriguez JP, Levine JM (2011) The RE1 binding protein REST regulates oligodendrocyte differentiation. *J Neurosci* 31(9):3470–3483.
24. Margueron R, Reinberg D (2011) The Polycomb complex PRC2 and its mark in life. *Nature* 469(7330):343–349.
25. Sher F, et al. (2008) Differentiation of neural stem cells into oligodendrocytes: involvement of the polycomb group protein Ezh2. *Stem Cells* 26(11):2875–2883.
26. Seong I, et al. (2009) Huntingtin facilitates polycomb repressive complex 2. *Hum Mol Genet*. doi:10.1093/hmg/ddp524.
27. Thakurela S, et al. (2016) The transcriptome of mouse central nervous system myelin. *Sci Rep* 6(1):25828.
28. Moreau-Fauvarque C, et al. (2003) The transmembrane semaphorin Sema4D/CD100, an inhibitor of axonal growth, is expressed on oligodendrocytes and upregulated after CNS lesion. *J Neurosci* 23(27):9229–9239.
29. Sprengelmeyer R, et al. (2014) The neuroanatomy of subthreshold depressive symptoms in Huntington's disease: a combined diffusion tensor imaging (DTI) and voxel-based morphometry (VBM) study. *Psychol Med* 44(9):1867–1878.
30. Edgar N, Sibille E (2012) A putative functional role for oligodendrocytes in mood regulation. *Transl Psychiatry* 2(5):e109–9.
31. Nave K-A, Ehrenreich H (2014) Myelination and oligodendrocyte functions in psychiatric diseases. *JAMA Psychiatry* 71(5):582–584.
32. Shen X, et al. (2017) Subcortical volume and white matter integrity abnormalities in major depressive disorder: findings from UK Biobank imaging data. *Sci Rep* 7(1):5547.
33. Birey F, et al. (2015) Genetic and Stress-Induced Loss of NG2 Glia Triggers Emergence of Depressive-like Behaviors through Reduced Secretion of FGF2. *Neuron* 88(5):941–956.
34. Bohnen NI, Albin RL (2011) White matter lesions in Parkinson disease. *Nat Rev Neurol* 7(4):229–236.
35. Poudel GR, et al. (2014) White matter connectivity reflects clinical and cognitive status in Huntington's disease. *Neurobiol Dis* 65:180–187.
36. Tepper JM, Bolam JP (2004) Functional diversity and specificity of neostriatal interneurons. *Current Opinion in Neurobiology* 14(6):685–692.
37. Huang B, et al. (2015) Mutant huntingtin downregulates myelin regulatory factor-mediated myelin gene expression and affects mature oligodendrocytes. *Neuron* 85(6):1212–1226.
38. Koenning M, et al. (2012) Myelin gene regulatory factor is required for maintenance of myelin and mature oligodendrocyte identity in the adult CNS. *J Neurosci* 32(36):12528–12542.
39. Kim KH, Roberts CWM (2016) Targeting EZH2 in cancer. *Nat Med* 22(2):128–134.
40. Osipovitch M, et al. (2019) Human ESC-Derived Chimeric Mouse Models of Huntington's Disease Reveal Cell-Intrinsic Defects in Glial Progenitor Cell Differentiation. *Cell Stem Cell* 24(1):107–122.e7.
41. Humbert S (2010) Is Huntington disease a developmental disorder? *EMBO Rep* 11(12):899–899.
42. Arteaga-Bracho EE, et al. (2016) Postnatal and adult consequences of loss of huntingtin during development: Implications for Huntington's disease. *Neurobiol Dis* 96:144–155.
43. Nguyen GD, Gokhan S, Molero AE, Mehler MF (2013) Selective roles of normal and mutant huntingtin in neural induction and early neurogenesis. *PLoS ONE* 8(5):e64368.
44. Schneider S, et al. (2001) The AN2 protein is a novel marker for the Schwann cell lineage expressed by immature and nonmyelinating Schwann cells. *J Neurosci* 21(3):920–933.
45. Ribchester RR, et al. (2004) Progressive abnormalities in skeletal muscle and neuromuscular junctions of transgenic mice expressing the Huntington's disease mutation. 20(11):3092–3114.